Regulation of Apoptosis via the NFκB Pathway: Modeling and Analysis

Madalena Chaves,[1] Thomas Eissing,[2] and Frank Allgöwer[3]

[1] COMORE, INRIA, 2004 Route des Lucioles, BP 93, 06902 Sophia-Antipolis, France; `mchaves@sophia.inria.fr`
[2] Bayer Technologies Services GmbH, PT-AS Systems Biology, Germany `thomas.eissing@bayertechnology.com`
[3] Institute for Systems Theory and Automatic Control, University of Stuttgart, Pfaffenwaldring 9, 70550 Stuttgart, Germany; `allgower@ist.uni-stuttgart.de`

1 Introduction

Programmed cell death (or apoptosis) has an essential biological function, enabling successful embryonic development, as well as maintenance of a healthy living organism [6]. Apoptosis is a physiological process which enables an organism to remove unwanted or damaged cells. Malfunctioning apoptotic pathways can lead to many diseases, including cancer and inflammatory or immune system related problems. A family of proteins called caspases are primarily responsible for execution of the apoptotic process: basically, in response to appropriate stimuli, initiator caspases (for instance, caspases 8, 9) activate effector caspases (for instance, caspases 3, 7), which will then cleave various cellular substrates to accomplish the cell death process [22].

Nuclear factor κB (NFκB) is a transcription factor for a large group of genes which are involved in several different pathways. For instance, NFκB activates its own inhibitor (IκB) [14] as well as groups of pro-apoptotic and anti-apoptotic genes [21]. Among the latter, NFκB activates transcription of a gene encoding for inhibitor of apoptosis protein (IAP). This protein in turn contributes to downregulate the activity of the caspase cascade which forms the core of the apoptotic pathway [6, 8].

The canonical NFκB pathway is induced, among other stimuli, by the cytokine tumor necrosis factor α (TNFα) [21]. Binding of TNFα to death receptor TNFR1 forms a first complex which eventually activates NFκB. A second complex is later formed, which will activate the initiator caspase 8 [6], and hence activate the apoptotic process. The same signal (TNFα stimulation) thus triggers two parallel but contrary pathways: the pro-apoptotic caspase cascade and the anti-apoptotic NFκB-IκB-IAP pathway. These two pathways, together with the interactions among their components, form a

complex network which shapes the decision on cell survival or initiation of programmed cell death. To contribute to a better understanding of the role of NFκB in the regulation of apoptosis, we propose a qualitative study of this system and its dynamics, based on a discrete (Boolean) model of the complex network. This discrete model closely follows a continuous one, recently developed and studied in [23, 24]. The model integrates the well-known model for the NFκB pathway [17] and the caspase cascade [8].

Boolean models provide a convenient formalism to describe protein and gene networks [25]. The states of the network components (e.g., proteins or messenger RNAs) are characterized as "expressed" or "not expressed" and are represented by logical variables (with values 0 or 1). The interactions among the various components are classified as "inhibition" or "activation" links (these can generally be deduced from gene/protein expression data). Boolean models thus describe the network structure of a system without involving any kinetic details. The qualitative behaviour of a system can be seen as an emergent property of this structure. Boolean models are especially useful in the case of large networks [1, 9], for which kinetic parameters are often unknown, but qualitative properties such as generation of specific gene expression patterns, stability or multistability, and oscillatory modes can be studied. Several methods have been developed for analysis of discrete and qualitative models [2, 5, 7, 13, 26]. Using an approach which combines discrete rules with continuous degradation rates, our model reproduces many of the known properties of the system, notably the oscillatory dynamics that can be induced by the NFκB-IκB negative feedback loop [14, 15, 19]. We explore different configurations for the network structure and predict its effects on the decision between cell survival or apoptosis.

2 The Model

The network of interactions among the NFκB pathway and the apoptosis signaling cascade to be studied here is shown in Fig. 1. The various components of the network (here messenger RNAs, proteins, or protein complexes) form the set of variables or nodes (X_i, $i = 1, \ldots, n$) of the Boolean model. The system will evolve according to a set of logical rules which are deduced from the interactions or links depicted in the schematic diagram of Fig. 1. The interactions among nodes can be classified as "activation" or "inhibition" links: a directed arrow $X_i \rightarrow X_j$ means that a high concentration of component X_i activates component X_j, while the symbol $X_i \dashv X_j$ means that a high concentration of component X_i inhibits X_j.

The components in our model and the activation or inhibition links among them are based on existing literature data. For general aspects, the reviews [6, 21] were used. However, some pathways of regulation among the NFκB pathway and the caspase cascade are not yet clear, and more work is needed to understand how these two signaling pathways are interconnected. In this chapter, we aim to investigate and test several possible hypotheses for
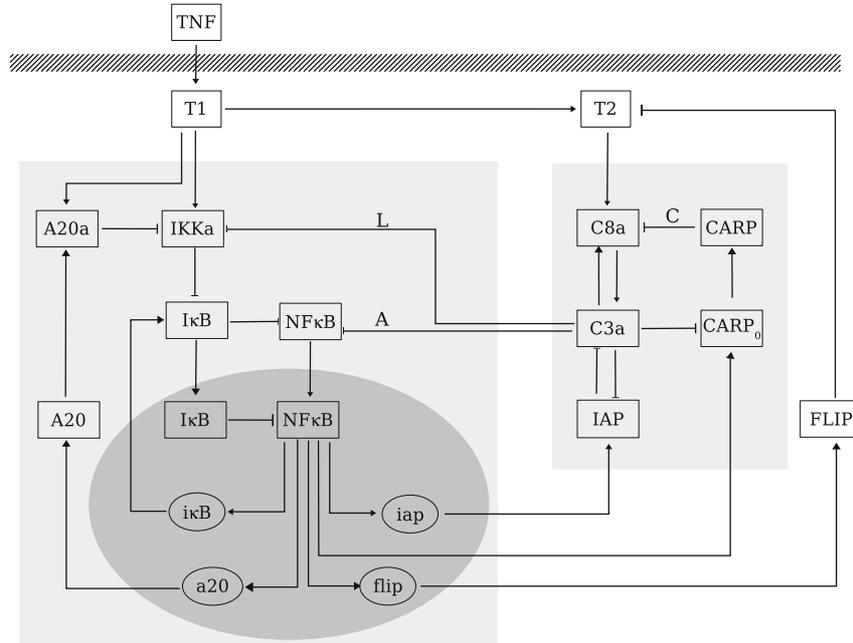
Fig. 1. Schematic diagram of the NFκB pathway and the caspase cascade (light shaded regions). The oval dark grey shaded region represents the cellular nucleus. Both pathways are activated by binding of TNFα to death receptor TNFR1 (the resulting complex is represented simply by the rectangle TNF). Messenger RNAs are represented by ellipses, while transcription factors, caspases, and other proteins are represented by squares. To study the interconnections between the two pathways, four network variants, based on different combinations of the links A, L, and C, will be analysed and compared (see Table 2).

the combined network structure. We will consider four model variants and try to discriminate between them by comparing our numerical analysis with experimental data from the literature. The four network variants (see Table 2) are based on different combinations of three links (A, L, C in Fig. 1) which have been suggested but are not fully established in the apoptosis literature.

The NFκB pathway follows very closely the model presented in [17]. Stimulation of death receptors with TNFα leads (see for instance [6]), first, to the formation of a complex I (T_1 in Fig. 1) which will recruit and activate inhibitor of IκB kinases (IKK). Inhibitor of NFκB, or IκB, acts by binding to NFκB molecules and preventing their transcriptional function. Active IKK (IKKa) phosphorylates IκB which releases NFκB, thus enabling its translocation to the nucleus and transcription of NFκB-dependent genes, including genes for inhibitor of apoptosis protein (iap), inhibitor of NFkB (iκB), a protein associated with inhibition of complex T_2 (flip), and a protein regulating IKK activity (a20) [21]. Transcription of IκB mRNA generates a negative feedback

loop in the NFκB pathway [14, 20], which may lead to oscillatory behaviour in NFκB and IκB concentrations [19]. In a second step, after dissociation of components of complex I from the death receptor, a second complex is formed (T_2 in Fig. 1) which will recruit and activate initiator caspase 8 (C8a). As a result of the signaling cascade [8, 22], effector caspase 3 is also activated (C3a). Thus, complex T_1 activates the anti-apoptotic pathway and, after a certain delay, complex T_2 activates the pro-apoptotic pathway.

Two well-documented points of regulation of the apoptotic pathway by NFκB are inhibition of C3a by IAP and regulation of complex T_2 by FLIP [6]. Active caspase 8 was found to be negatively regulated by caspase-8 and caspase-10-associated RING proteins (CARPs) [18], which seem to play an analogous role to IAP's, but are less well studied. It was found that CARPs are overexpressed in tumors, and that their suppression leads to restoration of the apoptotic pathway, with the CARP being rapidly cleaved. In addition, it was observed that inhibitors of caspase 3 block CARP cleavage. In our model, we introduced CARP and a pre-complex $CARP_0$, which is inhibited by C3a. Inhibition by C3a is, however, not sufficient to control CARP, and there are probably other regulators. Since CARP plays a similar role to caspases 8 and 10, as IAP plays to caspases 3 and 9 (and in the absence of further details), we assume that the pre-complex $CARP_0$ is also regulated by a product of the NFκB pathway.

The points where the caspase cascade influences the NFκB pathway are less well documented. We will use our model to test different hypotheses by studying and comparing the network dynamics for the following cases (see also Table 2): inhibition of IKKa (link L) and/or NFκB (link A) by C3a, or neither of these links present.

To obtain the logical rules shown in Table 1, some simplifications of the biological processes were inevitably introduced. For instance, the bound complex NFκB−IκB (either in the cytoplasm or in the nucleus) was not explicitly considered in the system, but was simply treated as an inhibition effect: the rule for NFκB says that it vanishes whenever IκB is expressed. Thus, any state with NFκB = 0 and IκB = 1 represents in fact a high concentration of bound complex NFκB − IκB, while any state with NFκB = 1 and IκB = 0 represents a high concentration of free NFκB and low concentration of free IκB. To translate our diagram into a set of logical rules, the convergence of two or more arrows (either activation or inhibition) at the same node was always treated as a logical AND, except in three cases: IκB, IAP, and $CARP_0$. For these proteins, the overall effect was treated as an AND in the presence of TNF stimulation, but treated as an OR in the absence of TNF. These three proteins represent inhibitors whose levels should be stable in the absence of any stimulus [8]: IAP and $CARP_0$ (or CARP) should be effective inhibitors of the caspases, and IκB should be at approximately constant levels to control NFκB transcriptional activity. In contrast, with TNF stimulation, the degradation rates of these proteins can vary and lead to rapid changes in their concentrations (different degradation rates in the presence or absence of TNF

have been observed, notably for bound IκB [20]). For instance, under TNF treatment, the rule for inhibition of NFκB is simplified to IκB$^+$= [iκB and not IKKa]. Suppose that IKK becomes activated at time t_1, that is IKKa$(t_1) = 1$. Then, in the next iteration of the model, the IκB rule implies that IκB will degrade very fast, with IκB$(t_1+\Delta) = 0$. In contrast, in the absence of the TNF stimulus, the rule is IκB$^+$= [iκB or not IKKa]. If IKK becomes active at time t_1, one has IκB$(t_1 + \Delta) = $ iκB(t_1), meaning that IκB is only rapidly degraded if no more of its messenger RNA is available. A similar reasoning justifies the rules for IAP and CARP$_0$. The rules for these three proteins with inhibiting roles reflect the fact that their degradation rates, and hence turnover, can be much faster in response to TNF stimulation.

3 Analysis of Boolean Models

Boolean networks are a representation of a system, consisting of a set of n variables or nodes $X = (X_1, \ldots, X_n)$, together with a set of logical rules $(F_i(X), i = 1, \ldots, n)$ describing the evolution of the system from the current state (X_i at time t) to the next state (X_i at time $t + \Delta$). The variables or nodes take values in the discrete set $\{0, 1\}$, where 1 (resp., 0) denotes the "expressed" (resp., "not expressed") state of the node. The associated rules are typically a composition of logical OR and AND functions, which can be determined from gene/protein expression patterns (from Western blots or microarray data, for instance). The set of rules F_i given in Table 1 for the NFκB pathway and the caspase cascade is a translation of the diagram shown in Fig. 1. The temporal evolution of the system, $X(t)$, $t \in (0, \infty)$, is determined by successively iterating the logical rules F_i, for which several algorithms are available. Synchronous algorithms assume that all nodes are simultaneously updated:

$$X_i^+ \; = \; F_i(X_1, \ldots, X_n), \quad i = 1, \ldots, n, \tag{1}$$

where $X_i \in \{0, 1\}$, $X = (X_1, \ldots, X_n)$ denotes the state of the system at time t, and $X^+ = (X_1^+, \ldots, X_n^+)$ denotes the next state (at $t + \Delta$). Alternatively, with asynchronous algorithms, at each iteration the nodes are sequentially updated, according to a given order (which can be prespecified or randomly chosen).

Discrete models focus on the structure of the network (links), thus offering a more qualitative description of the system's dynamics. Continuous models may offer more detailed descriptions of a system, but they also have the disadvantage of involving a large set of kinetic parameters, many of which are unknown. A method for analysis of Boolean models was introduced in [12, 13], which provides a bridge between discrete and continuous approaches. In this method, each node X_i of the network is represented by one continuous variable (x_i) and one discrete variable (X_i, as before). The continous variables are

Table 1. Boolean rules for the model of regulation of apoptosis via the NFκB pathway. TNF is a constant input. Identification of the nodes is given in the text. The letter "a" juxtaposed to a variable name denotes the active form of a molecule. The subscript "nuc" denotes the given component in the cellular nucleus. Alternative rules are given for the presence/absence of links A, C, L.

Node	Boolean rule
$T_1{}^+$	TNF
$T_2{}^+$	T_1 and not FLIP
IKKa$^+$	{L} T_1 and not A20a and not C3a {no L} T_1 and not A20a
NFκB$^+$	{A} not IκB and not C3a {no A} not IκB
NFκB$_{\text{nuc}}^+$	NFκB and not IκB$_{\text{nuc}}$
iκB$^+$	NFκB$_{\text{nuc}}$
IκB$^+$	[T_1 and (iκB and not IKKa)] or [not T_1 and (iκB or not IKKa)]
IκB$_{\text{nuc}}^+$	IκB
a20$^+$	NFκB$_{\text{nuc}}$
A20$^+$	a20
A20a$^+$	T_1 and A20
iap$^+$	NFκB$_{\text{nuc}}$
IAP$^+$	[T_1 and (iap and not C3a)] or [not T_1 and (iap or not C3a)]
flip$^+$	NFκB$_{\text{nuc}}$
FLIP$^+$	flip
C3a$^+$	not IAP and C8a
C8a$^+$	{C} not CARP and (C3a or T_2) {no C} C3a or T_2
CARP$_0^+$	[T_1 and (NFκB$_{\text{nuc}}$ and not C3a)] or [not T_1 and (NFκB$_{\text{nuc}}$ or not C3a)]
CARP$^+$	CARP$_0$

governed by ordinary differential equations, which combine a synthesis rate (based on its Boolean rule) and a linear degradation rate:

$$\frac{d\,x_i}{dt} = -a_i x_i + b_i F_i(X_1, X_2, \ldots, X_n), \quad i = 1, \ldots, n. \tag{2}$$

At each instant t, the discrete variable X_i is defined as a function of the continuous variable according to a threshold value of its maximal concentration:

$$X_i(t) = \begin{cases} 0, \ x_i(t) \le \theta_i \frac{b_i}{a_i} \\ 1, \ x_i(t) > \theta_i \frac{b_i}{a_i} \ , \end{cases} \tag{3}$$

where $\theta_i \in (0,1)$ represents the fraction of maximal concentration which is necessary for component X_i to become "active" and perform its biological functions. Initial conditions are equal for discrete and continuous variables: $X_i(0) = x_i(0)$. It is easy to see that the hypercube $[0, b_1/a_1] \times \cdots \times [0, b_n/a_n]$ is an invariant set for system (2). The continuous variables denote concentrations of molecules; they are translated into a Boolean 0/1 response according to θ_i. The discrete variables X_i represent expression (1) or not expression (0)

of species i, according to whether its continuous concentration x_i is above or below the threshold $\theta_i b_i / a_i$. Letting the parameters a_i, b_i, and θ_i be specific for each node i allows us to study different time scales for different biological processes (for instance, transcription, translation, or post-translational processes, as in [5]), or investigate the relative turnover rates of two molecules. Similar piecewise linear systems have also been studied in [7, 26].

3.1 Steady States

The steady states of a Boolean model are given by all the possible solutions X^* of the equations:

$$X_i^* = F_i(X_1^*, \ldots, X_n^*), \quad i = 1, \ldots, n.$$

It is easy to see that any steady state of the Boolean model yields a steady state of the piecewise linear equations (2), since

$$\frac{d\, x_i}{dt} = 0 \iff x_i = \frac{b_i}{a_i} F_i(X_1, X_2, \ldots, X_n), \ i = 1, \ldots, n,$$

independently of θ_i. Because the right-hand side of this equation is discontinuous, it is difficult to provide general results on the existence and uniqueness of solutions for system (2) (see for instance [3] and [11]). In view of this difficulty, in the present study we will assume that trajectories are well defined and analyze their dynamical behavior.

For the model of Table 1, the steady states depend on the value of TNF (see Table 2). It is not difficult to check that (both with and without link A) there are exactly two distinct steady states when TNF = 0, characterized by the presence or absence of caspases 3 and 8, and hence corresponding to the survival or apoptotic responses (nodes not indicated below are zero):

$$(\mathrm{Ap}_0) \ \ \mathrm{T}_1 = \mathrm{T}_2 = 0, \ \mathrm{C3a} = \mathrm{C8a} = 1, \ \mathrm{I}\kappa\mathrm{B} = \mathrm{I}\kappa\mathrm{B}_{\mathrm{nuc}} = 1, \tag{4}$$
$$(\mathrm{Lf}_0) \ \ \mathrm{T}_1 = \mathrm{T}_2 = 0, \ \mathrm{I}\kappa\mathrm{B} = \mathrm{I}\kappa\mathrm{B}_{\mathrm{nuc}} = 1, \ \mathrm{CARP}_0 = \mathrm{CARP} = \mathrm{IAP} = 1.$$

This is in agreement with the idea that, under typical conditions, the cell should be capable of stably maintaining either an apoptotic or a survival

Table 2. Steady states of the Boolean model, for each model variant, in the presence and absence of TNF.

Model	Links	TNF = 0	TNF = 1	Oscillations?
I	A, C, no L	Ap_0, Lf_0	Ap_1	Yes
II	L, C, no A	Ap_0, Lf_0	—	Yes
III	C, no A, no L	Ap_0, Lf_0	—	Yes
IV	L, no A, no C	Ap_0, Lf_0	—	Yes

state [8, 4]. If TNF = 1, there is only one possible steady state for models with link A:

$$(Ap_1) \qquad T_1 = T_2 = 1, \; C3a = C8a = 1. \qquad (5)$$

For models with no link A, there is no possible steady state when TNF = 1, and there are only periodic orbits of period higher than 1.

Therefore, during TNF treatment, models with link A may at any time make a decision towards the apoptotic pathway, while models with no link A will exhibit oscillatory behaviour and can only make a decision when TNF treatment ceases. Upon removal of TNF stimulation, trajectories of system (2) may be expected to converge to either the apoptotic or survival state. The choice of one or the other state will depend on the initial condition and the set of parameters a_i, b_i, and θ_i. Since these parameters are very likely to vary from cell to cell, it is reasonable to consider several (randomly chosen) sets of parameters and then compute the probability of convergence to each steady state. To examine the dynamics of system (2), and its dependence on parameters and the structure of the network of interactions, several numerical studies were performed, as described next.

3.2 Numerical Experiments

To test the model and analyse the effects of links A and L (Fig. 1), system (2) was simulated several times, with randomly chosen sets of parameters. For simplicity, the synthesis rates and threshold constants were fixed ($b_i = 1$ and $\theta_i = 0.5$ for all i), and only parameters a_i were allowed to vary, chosen from a uniform distribution in the interval $[1/3, 3]$ (h^{-1}). This seems reasonable, as the degradation rates used in [17] are roughly between 0.5 and 4 h^{-1}. Observe that a_i plays a double role: it represents a degradation rate, but also defines the 0/1 threshold concentration ($0.5/a_i$). Hence, high degradation rates also imply that a lower concentration is needed to achieve the 0/1 transition. Different durations of TNF stimulation were considered, namely: 2, 6, 11, 16, and 21 hours. For these simulations, one initial condition was chosen: IκB(0) = 1 and all other nodes set to zero. This is based on a natural physiological starting point of the system: previous to stimulation, IKK is in its inactive form, while IκB is bound to NFκB, preventing transcriptional activity. Caspases reside in the cytosol in dormant forms [22].

To understand the importance of the links A, C, and L (the least well documented), four variants of the model depicted in Fig. 1 are compared: (I) links A and C present, (II) links L and C present, (III) only link C present, and (IV) only link L present (as listed in Table 2). The first three variants aim at comparing the effects of links A and L, and the last aims at evaluating the effect of link C. Other alternatives gave similar results (for example, a model with all three links gave results very similar to I) and thus are not detailed here. For each variant, the response of the system to each of the five TNF

durations was simulated 500 times. Since different sets of parameters $\{a_i\}$ introduce different time scales, variations in the dynamics from one simulation to another are expected. These variations may also be interpreted as a result of natural variability in biological systems. The average response over the 500 simulations will then yield the probability of the system converging towards each of the steady states.

Other open questions that may be studied with our model include competition between the pro- and anti-apoptotic pathways and the point of irreversibility of the apoptotic decision. For instance, how long after caspase activation is recovery from the apoptotic pathway still possible [22]? To address these questions, numerical experiments were conducted by letting NFκB(0) = 1, setting all others to zero, and maintaining C3a(t) = 1 for durations of 10, 30, 60, and 360 minutes.

For analysis of the numerical results, a "peak" in the trajectory of node X_j will be defined as a time interval $[T_0, T_1]$, during which $X_j(t) = 1$, and such that $X_j(T_0 - \Delta) = X_j(T_1 + \Delta) = 0$. The period of oscillations is calculated as the average time interval between the onset of two consecutive peaks, i.e.,

$$\text{Period} = \frac{1}{N_p - 1} \sum_{i=2}^{N_p} T_{0,i} - T_{0,i-1},$$

where N_p is the number of peaks observed during the simulation time.

4 Results and Discussion

In the numerical simulations, it is observed that, once TNF stimulation ceases, a steady state pattern is always achieved, corresponding to either the apoptosis or survival states (4), (5). In the former case IκB is bound to NFκB, so that mRNAs and proteins downstream of NFκB are not expressed, and the cell has chosen the apoptotic pathway. The latter case represents survival of the cell, with IAP stably expressed preventing C3a activation, and CARP preventing C8a activation (see Fig. 2). In the presence of TNF stimulation, IκB, NFκB, and its dependent mRNAs/proteins may exhibit oscillatory dynamics, as observed experimentally in [14, 19]. In fact, computation of steady states shows that the models with no link A have no alternative but to exhibit oscillatory behaviour in the presence of TNF, since no possible steady states exist (except possible special solutions of the associated differential inclusion). The oscillatory behaviour (see analysis below) is in very good agreement with the experimental data reported in [19].

Qualitatively, all model variants respond in a similar fashion to TNF stimulation. As the stimulus duration increases, more cells choose the apoptotic pathway. Testing the four model variants shows that link A is very strong: not surprisingly, models with link A favour the apoptotic pathway, with 80% of cells reaching the apoptotic state, as opposed to around 50% or 40% in
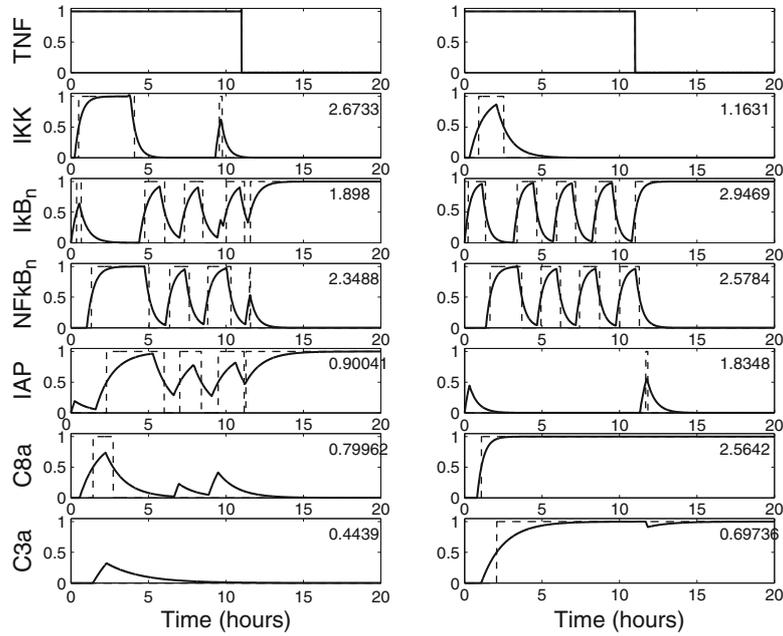
Fig. 2. Example of network dynamics with the hybrid model (variant II), corresponding to cell survival (left) or apoptosis (right) solution. Numbers indicate the degradation rates for these numerical experiments. Solid lines represent normalized continuous variables (x_i) and dashed lines represent discrete variables (X_i).
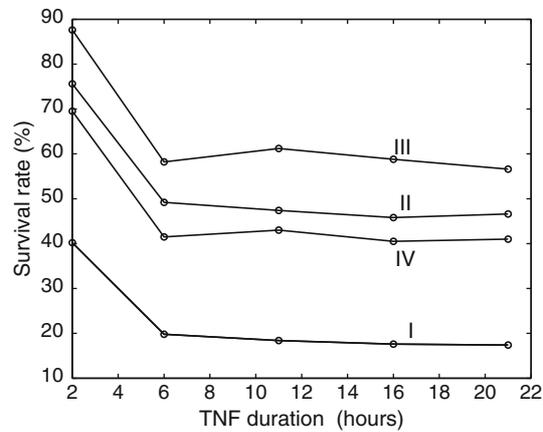

Fig. 3. Percentage of surviving cells for the four model variants.

models II and IV, or 30% in the model with only link C (which favours the anti-apoptotic pathway) (Fig. 3). These values appear to be in agreement with experimental data: Rehm et al. [22] report that, for 8 hour treatments with
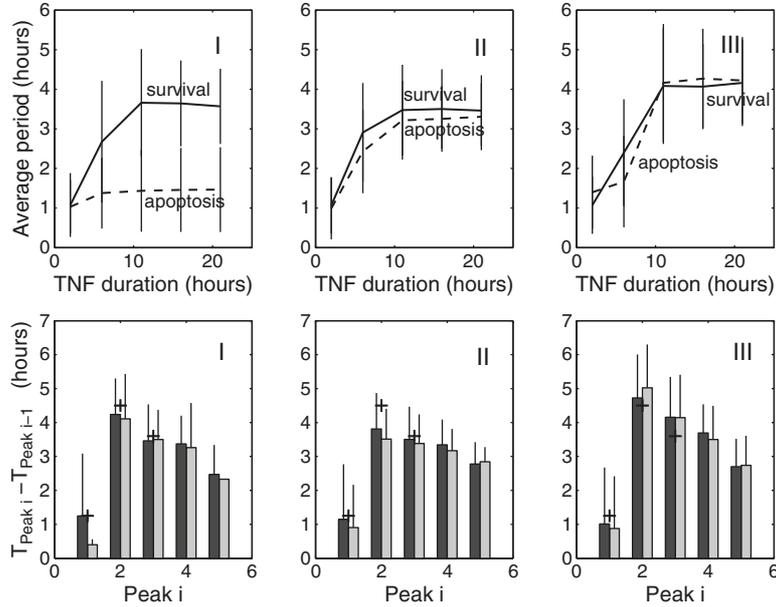
Fig. 4. Top row: Average period of nuclear IκB oscillations for apoptotic or surviving cells, as a function of TNF stimulus duration. Vertical lines represent standard deviation over the 500 numerical experiments. Bottom row: Relative timing of sucessive peaks in IκB oscillations, for apoptotic (grey) or surviving (black) cells. The "+" signs mark the experimental peak timing in [19].

high and low concentrations of TNFα, the percentage of cells undergoing activation of effector caspases was, respectively, 86% and 24%. The numerical experiments with our model capture the response to high (or significant) concentrations of TNFα, so variants I (followed by II and IV) are closer to the real system.

Quantitative analysis of the oscillatory behaviour reveals some interesting facts (Fig. 4). To characterize the oscillatory dynamics, the following quantities were computed for nuclear IκB: period of oscillations (approximated), number of peaks, and relative timing between peaks. First, in all cells oscillations cease when TNF stimulation ceases, in agreement with observations. Second, the timing of successive peaks is also in remarkable quantitative agreement with experimental data [19], see Fig. 4 (bottom row). The first peak in nuclear IκB concentration was observed about 72 minutes from the start of TNF stimulation, and the second peak appears about 4 hours later, very close to the 75 minutes and 4.5 hours reported in [19]. It is striking that the time span of the first peak is typically longer than that of the following peaks, and that the time lapse between consecutive peaks decreases (see Figs. 2, 4). Third, the average period of oscillations is fairly constant, but "depends" on the apoptosis/survival decision. Statistical analysis of the period of oscillations

(calculated as indicated in Section 3.2) in nuclear IκB indicates that there is a natural period (for TNF treatment longer than 3 hours) for cells that eventually survived. This period is about 3.5 ± 1 hours for models I, II, and IV, and slightly higher at 4 ± 1 hours for model III. In contrast, for cells that chose the apoptotic pathway, the period of oscillations can be much smaller. For models with link A, essentially no oscillations are observed in apoptotic cells (Fig. 4, top, left): this is because cell death is decided very early on, with link A immediately preventing any further NFκB activity. For model II (links C and L only), oscillations are observed in apoptotic cells with a natural period which is lower (about 3 ± 1 hours) than that for surviving cells (Fig. 4, top, middle). Results for model IV (not shown) are quite similar to those of model II. For model variant III, there is no difference between observed periods (Fig. 4, top, right). These results provide indications for discriminating between the four model variants and also suggest that the period of oscillations may play a role in the survival/apoptosis decision: lower periods/higher frequencies would lead towards the apoptotic pathway. A similar result has been reported, for instance, in the p53-Mdm2 system [16], where more peaks (higher frequency) were detected in response to higher (and more damaging) γ-irradiation doses. The p53-Mdm2 system also contains a negative feedback loop similar to the NFκB-IκB loop.

To address the question of irreversibility of the apoptotic decision, we checked the capacity of the network to recover from overexpression of active caspase 3. Fixing node C3a at its maximal value for intervals of 10, 30, 60, and 360 minutes (that is setting discrete C3a$(t) = 1$, for $t < 10$, 30, 60, or 360), we calculated the percentage of surviving cells. With model I there are no surviving cells after 1 hour of C3a overexpression but, with model II or IV, this percentage drops very fast from 45% to 30% survival at 1 hour overexpression and remains at this value for continued C3a overexpression (see Fig. 5). This suggests that a significant percentage of cells can still invert the apoptotic
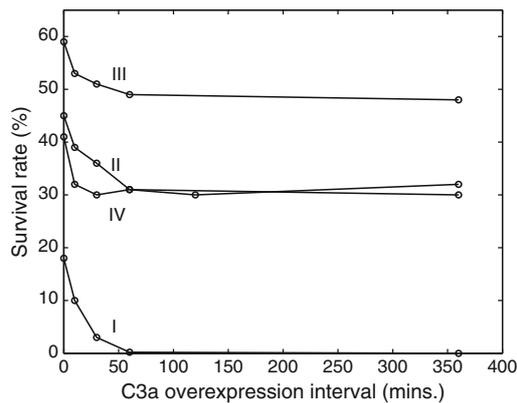

Fig. 5. Percentage of surviving cells under increasing intervals of C3a overexpression for the four model variants and TNF treatment for 16 hours.

decision, while for the largest part (70% of all cells) the apoptotic pathway is chosen early on, within an hour of TNF stimulation. Not surprisingly, examination of the relative values of the parameters a_i shows that two thirds of cells that were able to recover from the apoptotic pathway had degradation rates for C3a higher than those for NFκB or IκB.

Based on our study of regulation of apoptosis and the NFκB pathway, it seems clear that the links A and L play quite important roles, and at least one of these should definitely be included for faithful modeling of apoptosis via TNF receptors. This eliminates model III. Both links contribute to the same physiological function: downregulation of NFκB transcriptional activity. However, link A (direct inhibition of NFκB by C3a) achieves this objective in a much faster way than link L ("indirect" inhibition of NFκB by C3a, through complex IKK). The essential difference between models I and II is thus the length of the pathway representing inhibition of NFκB by C3a. The shorter path (model I, with link A) leads to much higher apoptosis rates than the longer path (models II or IV, with link L). The shorter path also renders recovery from the apoptosis pathway practically impossible, with apoptosis rates higher than 95% after only half an hour with C3a overexpression (Fig. 5). The longer path allows a higher recovery rate from the apoptotic pathway, although the probability of apoptosis does not increase above 70%, even after 6 hours of C3a overexpression. Recent experimental evidence [10] points to the existence of a link L, that is, caspases are responsible for cleavage or degradation of (parts of) complex IKK. To further discriminate between a short or long pathway for the influence of caspases on the NFκB pathway, the results shown in Fig. 4 suggest the following experiment. First, measure the period of oscillations during TNF stimulation and then monitor cells for some time after TNF removal. Next, compare the frequency of oscillations in cells that survive and in cells that eventually go through the apoptotic program. If the frequency of oscillations is similar for both groups of cells, or slightly higher in apoptotic cells, then model II (longer pathway) provides a better description of the system. If oscillations stopped after a short time interval (as compared to TNF duration) in apoptotic cells, then model I (shorter pathway) should be chosen.

5 Conclusion

The present study illustrates the usefulness of Boolean and piecewise linear models in the analysis of large complex networks. The qualitative dynamics that emerges from the network structure was studied, leading to predictions on the response to increasing duration of stimulation, response to overexpression of a given protein, or indication of which links/interactions play crucial roles in the regulation of apoptosis. Some quantitative aspects were also analyzed, such as the probabilities of survival or apoptosis and the frequency/period of oscillations, and were shown to be in remarkable agreement with experimental

data. Many other questions can be examined in this hybrid framework: for instance, extending the set of parameters (degradation and synthesis rates, threshold concentrations) and varying the relative strengths of anti- and pro-apoptotic links will lead to more refined models, capturing a wider range of kinetic variability. Although writing the logical rules requires some simplifications of the biological processes, discrete and hybrid models retain the essential qualitative properties of the network. The effect of the network structure on the qualitative dynamics of the system can be easily studied, even when kinetic details are not well known. This class of models can thus be a powerful method to generate predictions and test new hypotheses for complex biological networks.

Acknowledgments

References

1. R. Albert and H.G. Othmer. The topology of the regulatory interactions predicts the expression pattern of the *drosophila* segment polarity genes. *J. Theor. Biol.*, 223:1–18, 2003.
2. G. Bernot, J.-P. Comet, A. Richard, and J. Guespin. Application of formal methods to biological regulatory networks: extending Thomas' asynchronous logical approach with temporal logic. *J. Theor. Biol.*, 229:339–347, 2004.
3. R. Casey, H. de Jong, and J.L. Gouzé. Piecewise-linear models of genetic regulatory networks: equilibria and their stability. *J. Math. Biol.*, 52:27–56, 2006.
4. M. Chaves, T. Eissing, and F. Allgöwer. Bistable biological systems: a characterization through local compact input-to-state stability. *IEEE Trans. Automat. Control*, 53:87–100, 2008.
5. M. Chaves, E.D. Sontag, and R. Albert. Methods of robustness analysis for boolean models of gene control networks. *IEE Proc. Syst. Biol.*, 153:154–167, 2006.
6. N.N. Danial and S.J. Korsmeyer. Cell death: critical control points. *Cell*, 116: 205–216, 2004.
7. H. de Jong, J.L. Gouzé, C. Hernandez, M. Page, T. Sari, and J. Geiselmann. Qualitative simulation of genetic regulatory networks using piecewise linear models. *Bull. Math. Biol.*, 66:301–340, 2004.
8. T. Eissing, H. Conzelmann, E.D. Gilles, F. Allgöwer, E. Bullinger, and P. Scheurich. Bistability analysis of a caspase activation model for receptor-induced apoptosis. *J. Biol. Chem.*, 279:36892–36897, 2004.
9. A. Fauré, A. Naldi, C. Chaouiya, and D. Thieffry. Dynamical analysis of a generic boolean model for the control of the mammalian cell cycle. *Bioinformatics*, 22(14):e124–e131, 2006.
10. C. Frelin, V. Imbert, V. Bottero, N. Gonthier, A.K. Samraj, K. Schulze-Osthoff, P. Auberger, G. Courtois, and J.F. Peyron. Inhibition of the NF-κB survival pathway via caspase-dependent cleavage of the IKK complex scaffold protein and NF-κB essential modulator NEMO. *Cell Death Differ.*, 15:152–160, 2008.

11. T. Gedeon. Attractors in continuous-time switching networks. *Communications on Pure and Applied Analysis*, 2:187–209, 2003.

12. L. Glass. Classification of biological networks by their qualitative dynamics. *J. Theor. Biol.*, 54:85–107, 1975.

13. L. Glass and S.A. Kauffman. The logical analysis of continuous, nonlinear biochemical control networks. *J. Theor. Biol.*, 39:103–129, 1973.

14. A. Hoffmann, A. Levchenko, M.L. Scott, and D. Baltimore. The IκB-NFκB signaling module: temporal control and selective gene activation. *Science*, 298:1241–1245, 2002.

15. A.E.C. Ihekwaba, D. Broomhead, R. Grimley, N. Benson, and D.B. Kell. Sensitivity analysis of parameters controlling oscillatory signalling in the NF-κB pathway: the roles of IKK and IκBα. *IEE Syst. Biol.*, 1:93–103, 2004.

16. G. Lahav, N. Rosenfeld, A. Sigal, N. Geva-Zatorsky, A.J. Levine, M. Elowitz, and U. Alon. Dynamics of the p53-Mdm2 feedback loop in individual cells. *Nat. Genetics*, 36:147–150, 2004.

17. T. Lipniacki, P. Paszek, A.R. Brasier, B. Luxon, and M. Kimmel. Mathematical model of NFκB regulatory module. *J. Theor. Biol.*, 228:195–215, 2004.

18. E.R. McDonald and W.S. El-Deiry. Suppression of caspase-8 and -10-associated RING proteins results in sensitization to death ligands and inhibition of tumor cell growth. *Proc. Natl. Acad. Sci. USA*, 101:6170–6175, 2004.

19. D.E. Nelson, A.E.C. Ihekwaba, M. Elliott, J.R. Johnson, C.A. Gibney, B.E. Foreman, G. Nelson, V. See, C.A. Horton, D.G. Spiller, S.W. Edwards, H.P. McDowell, J.F. Unitt, E. Sullivan, R. Grimley, N. Benson, D. Broomhead, D.B. Kell, and M.R.H. White. Oscillations in NF-κB signaling control the dynamics of gene expression. *Science*, 306:704–708, 2004.

20. E.L. O'Dea, D. Barken, R.Q. Peralta, K.T. Tran, S.L. Werner, J.D. Kearns, A. Levchenko, and A. Hoffmann. A homeostatic model of IκB metabolism to control constitutive NFκB activity. *Mol. Syst. Biol.*, 3:111, 2007.

21. N.D. Perkins. Integrating cell-signalling pathways with NF-κB and IKK function. *Nat. Rev. Mol. Cell Biol.*, 8:49–62, 2007.

22. M. Rehm, H. Düßmann, R.U. Jänicke, J.M. Tavaré, D. Kögel, and J.H.M. Prehn. Single-cell fluorescence resonance energy transfer analysis demonstrates that caspase activation during apoptosis is a rapid process. *J. Biol. Chem.*, 277:24506–24514, 2002.

23. M. Schliemann. Modelling and experimental validation of TNFα induced pro- and antiapoptotic signalling. Master's thesis, University of Stuttgart, Germany, 2006.

24. M. Schliemann, T. Eissing, P. Scheurich, and E. Bullinger. Mathematical modelling of TNF-α induced apoptotic and anti-apoptotic signalling pathways in mammalian cells based on dynamic and quantitative experiments. In *Proc. 2nd Int. Conf. Foundations Systems Biology in Engineering (FOSBE), Stuttgart, Germany*, pages 213–218, 2007.

25. R. Thomas. Boolean formalization of genetic control circuits. *J. Theor. Biol.*, 42:563–585, 1973.

26. R. Thomas, D. Thieffry, and M. Kaufman. Dynamical behaviour of biological regulatory networks - i. biological rule of feedback loops and practical use of the concept of the loop-characteristic state. *Bull. Math. Biol.*, 57:247–276, 1995.

Dynamics On and Of Complex Networks
Applications to Biology, Computer Science, and the
Social Sciences
Ganguly, N.; Deutsch, A.; Mukherjee, A. (Eds.)
2009, XIV, 305 p. 98 illus., Hardcover
ISBN: 978-0-8176-4750-6
A product of Birkhäuser Basel